Final results of the search for $\nu_\mu \rightarrow \nu_e$ oscillations with the OPERA detector in the CNGS beam

The OPERA collaboration

N. Agafonova,[a] A. Aleksandrov,[b] A. Anokhina,[c] S. Aoki,[d] A. Ariga,[e] T. Ariga,[e,f]
A. Bertolin,[g] C. Bozza,[h] R. Brugnera,[g,i] A. Buonaura,[b,j] S. Buontempo,[b]
M. Chernyavskiy,[k] A. Chukanov,[l] L. Consiglio,[b] N. D'Ambrosio,[m] G. De Lellis,[b,j]
M. De Serio,[n,o] P. del Amo Sanchez,[p] A. Di Crescenzo,[b,j] D. Di Ferdinando,[q]
N. Di Marco,[m] S. Dmitrievsky,[l] M. Dracos,[r] D. Duchesneau,[p] S. Dusini,[g]
T. Dzhatdoev,[c] J. Ebert,[s] A. Ereditato,[e] J. Favier,[p] R.A. Fini,[o] F. Fornari,[q,t]
T. Fukuda,[u] G. Galati,[b,j] A. Garfagnini,[g,i] V. Gentile,[v] J. Goldberg,[w] Y. Gornushkin,[l]
S. Gorbunov,[k] G. Grella,[h] A. M. Guler,[x] C. Gustavino,[y] C. Hagner,[s] T. Hara,[d]
T. Hayakawa,[u] A. Hollnagel,[s] B. Hosseini,[b,j,1] K. Ishiguro,[u] A. Iuliano,[j] K. Jakovcic,[z]
C. Jollet,[r] C. Kamiscioglu,[x,aa] M. Kamiscioglu,[x] S.H. Kim,[ab] N. Kitagawa,[u]
B. Klicek,[ac] K. Kodama,[ad] M. Komatsu,[u] U. Kose,[g,2] I. Kreslo,[e] F. Laudisio,[g,i]
A. Lauria,[b,j] A. Ljubicic,[z,3] A. Longhin,[g,i] P. Loverre,[y] A. Malgin,[a] M. Malenica,[z]
G. Mandrioli,[q] T. Matsuo,[ae] V. Matveev,[a] N. Mauri,[q,t] E. Medinaceli,[g,i,4] F. Meisel,[e]
A. Meregaglia,[r] S. Mikado,[af] M. Miyanishi,[u] F. Mizutani,[d] P. Monacelli,[y]
M.C. Montesi,[b,j] K. Morishima,[u] M.T. Muciaccia,[n,o] N. Naganawa,[u] T. Naka,[u]
M. Nakamura,[u] T. Nakano,[u] K. Niwa,[u] N. Okateva,[k] S. Ogawa,[ae] K. Ozaki,[d]
A. Paoloni,[ag] L. Paparella,[n,o] B.D. Park,[ab] L. Pasqualini,[q,t] A. Pastore,[o] L. Patrizii,[q]
H. Pessard,[p] D. Podgrudkov,[c] N. Polukhina,[k,ah] M. Pozzato,[q,t] F. Pupilli,[g]
M. Roda,[g,i,5] T. Roganova,[c] H. Rokujo,[u] G. Rosa,[y] O. Ryazhskaya,[a] O. Sato,[u]
A. Schembri,[m] I. Shakiryanova,[a] T. Shchedrina,[k] H. Shibuya,[ae] E. Shibayama,[d]

---

[1]Now at INFN Sezione di Cagliari.
[2]Now at CERN.
[3]Deceased.
[4]Now at Osservatorio Astronomico di Padova.
[5]Now at University of Liverpool.

T. Shiraishi,^{u} **S. Simone,**^{n,o} **C. Sirignano,**^{g,i} **G. Sirri,**^{q} **A. Sotnikov,**^{l} **M. Spinetti,**^{ag}
L. Stanco,^{g} **N. Starkov,**^{k} **S.M. Stellacci,**^{h} **M. Stipcevic,**^{ac} **P. Strolin,**^{b,j} **S. Takahashi,**^{d}
M. Tenti,^{q,6} **F. Terranova,**^{ai} **V. Tioukov,**^{b} **S. Vasina,**^{l,6} **P. Vilain,**^{aj} **E. Voevodina,**^{b}
L. Votano,^{ag} **J.L. Vuilleumier,**^{e} **G. Wilquet**^{aj} **and C.S. Yoon**^{ab}

^{a}*INR — Institute for Nuclear Research of the Russian Academy of Sciences,*
RUS-117312 Moscow, Russia

^{b}*INFN — Sezione di Napoli, I-80125 Napoli, Italy*

^{c}*SINP MSU — Skobeltsyn Institute of Nuclear Physics, Lomonosov Moscow State University,*
RUS-119991 Moscow, Russia

^{d}*Kobe University, J-657-8501 Kobe, Japan*

^{e}*Albert Einstein Center for Fundamental Physics, Laboratory for High Energy Physics (LHEP),*
University of Bern, CH-3012 Bern, Switzerland

^{f}*Faculty of Arts and Science, Kyushu University, J-819-0395 Fukuoka, Japan*

^{g}*INFN — Sezione di Padova, I-35131 Padova, Italy*

^{h}*Dipartimento di Fisica dell'Università di Salerno and "Gruppo Collegato" INFN,*
I-84084 Fisciano (Salerno), Italy

^{i}*Dipartimento di Fisica e Astronomia dell'Università di Padova, I-35131 Padova, Italy*

^{j}*Dipartimento di Fisica dell'Università Federico II di Napoli, I-80125 Napoli, Italy*

^{k}*LPI — Lebedev Physical Institute of the Russian Academy of Sciences,*
RUS-119991 Moscow, Russia

^{l}*JINR — Joint Institute for Nuclear Research, RUS-141980 Dubna, Russia*

^{m}*INFN — Laboratori Nazionali del Gran Sasso, I-67010 Assergi, L'Aquila, Italy*

^{n}*Dipartimento di Fisica dell'Università di Bari, I-70126 Bari, Italy*

^{o}*INFN — Sezione di Bari, I-70126 Bari, Italy*

^{p}*LAPP, Université Savoie Mont Blanc, CNRS/IN2P3,*
F-74941 Annecy-le-Vieux, France

^{q}*INFN — Sezione di Bologna, I-40127 Bologna, Italy*

^{r}*IPHC, Université de Strasbourg, CNRS/IN2P3, F-67037 Strasbourg, France*

^{s}*Hamburg University, D-22761 Hamburg, Germany*

^{t}*Dipartimento di Fisica e Astronomia dell'Università di Bologna, I-40127 Bologna, Italy*

^{u}*Nagoya University, J-464-8602 Nagoya, Japan*

^{v}*GSSI — Gran Sasso Science Institute, I-40127 L'Aquila, Italy*

^{w}*Department of Physics, Technion, IL-32000 Haifa, Israel*

^{x}*METU — Middle East Technical University, TR-06800 Ankara, Turkey*

^{y}*INFN — Sezione di Roma, I-00185 Roma, Italy*

^{z}*Ruder Bošković Institute, HR-10002 Zagreb, Croatia*

^{aa}*Ankara University, TR-06560 Ankara, Turkey*

^{ab}*Gyeongsang National University, 900 Gazwa-dong, Jinju 660-701, Korea*

^{ac}*Center of Excellence for Advanced Materials and Sensing Devices, Ruder Bošković Institute,*
HR-10002 Zagreb, Croatia

^{ad}*Aichi University of Education, J-448-8542 Kariya (Aichi-Ken), Japan*

^{ae}*Toho University, J-274-8510 Funabashi, Japan*

^{af}*Nihon University, J-275-8576 Narashino, Chiba, Japan*

---

^{6}Corresponding author.

^{ag} *INFN — Laboratori Nazionali di Frascati dell'INFN, I-00044 Frascati (Roma), Italy*
^{ah} *MEPhI — Moscow Engineering Physics Institute, RUS-115409 Moscow, Russia*
^{ai} *Dipartimento di Fisica dell'Università di Milano-Bicocca, I-20126 Milano, Italy*
^{aj} *IIHE, Université Libre de Bruxelles, B-1050 Brussels, Belgium*

  E-mail: tenti@bo.infn.it, vasina@jinr.ru

ABSTRACT: The OPERA experiment has discovered the tau neutrino appearance in the CNGS muon neutrino beam, in agreement with the 3 neutrino flavour oscillation hypothesis. The OPERA neutrino interaction target, made of Emulsion Cloud Chambers, was particularly efficient in the reconstruction of electromagnetic showers. Moreover, thanks to the very high granularity of the emulsion films, showers induced by electrons can be distinguished from those induced by π^0s, thus allowing the detection of charged current interactions of electron neutrinos. In this paper the results of the search for electron neutrino events using the full dataset are reported. An improved method for the electron neutrino energy estimation is exploited. Data are compatible with the 3 neutrino flavour mixing model expectations and are used to set limits on the oscillation parameters of the 3+1 neutrino mixing model, in which an additional mass eigenstate m_4 is introduced. At high Δm_{41}^2 ($\gtrsim 0.1$ eV^2), an upper limit on $\sin^2 2\theta_{\mu e}$ is set to 0.021 at 90% C.L. and $\Delta m_{41}^2 \gtrsim 4 \times 10^{-3}$ eV^2 is excluded for maximal mixing in appearance mode.

Contents

1 Introduction

The main goal of the OPERA experiment was the search for $\nu_\mu \to \nu_\tau$ oscillations in the region of squared mass difference pointed out by experiments on the atmospheric neutrinos through the observation of the tau neutrino appearance in a muon neutrino beam [1]. The OPERA apparatus [2] located at the Gran Sasso Underground Laboratory was exposed from 2008 to 2012 to the CERN Neutrinos to Gran Sasso (CNGS) muon neutrino beam [3, 4], produced at a distance of about 730 km. The analysis of a data set released in 2015 led to the identification of five tau neutrino candidates with an expected background of 0.25, thus excluding the no-oscillation hypothesis with a significance greater than 5σ [5]. The OPERA nuclear emulsion target also allows the identification of ν_e (or $\bar{\nu}_e$) charged current (CC) interactions. The outcome of the search for electron neutrinos in the data collected in 2008–2009 was reported in [6]. Here, we report the results of an improved analysis on the complete dataset, corresponding to 17.97×10^{19} p.o.t., which represents an increase of the exposure by a factor 3.4 with respect to the previous analysis. Data compared with the expectation from the 3 neutrino flavour oscillation model allow setting an upper limit on the ν_e appearance probability. Moreover, the hypothesis of a sterile neutrino, as hinted by LSND [7], MiniBooNE [8], reactor [9], and radio-chemical [10, 11] experiments, is tested. Limits on Δm_{41}^2 and $\sin^2 2\theta_{\mu e} = 4|U_{e4}|^2|U_{\mu4}|^2$ are derived.

2 The OPERA experiment

The detector was composed of two identical super modules, each consisting of a target section and a magnetic iron spectrometer. Each target section contained about 75000 Emulsion Cloud Chamber [12] modules, hereafter called bricks, for a total target mass

of about 1.25 kt. The bricks were arranged in vertical walls interleaved with planes of horizontal and vertical scintillator strips, which formed the Target Tracker (TT). Each brick consisted of 56 1-mm lead plates interspersed with 57 emulsion films. It had a section of 12.7×10.2 cm^2 and a thickness of 7.5 cm, which corresponds to $\sim$10 radiation lengths (X_0). A pair of emulsion films (Changeable Sheet or CS doublet) were packed and glued externally to the downstream face of each brick. The CS doublet acted as an interface between the cm-resolution TT and μm-resolution emulsion, thus triggering the film development. The spectrometer, instrumented with planes of Resistive Plate Chambers (RPC) and drift tube stations, provided the charge and momentum measurements of muons [13].

The CNGS beam was an almost pure muon neutrino beam having a mean energy of 17 GeV. The contaminations, in terms of CC interactions, of ν_e, $\bar{\nu}_e$ and $\bar{\nu}_\mu$ were 0.88%, 0.05% and 2.1%, respectively.

The TT hits of an event occurring on time with the CNGS beam were used to track charged particles in the target region and to provide a calorimetric energy measurement. The TT information was exploited to rank the bricks according to their probability to contain the neutrino interaction vertex [14]. The highest probability brick was extracted from the detector. The attached CS doublet was scanned and the pattern of reconstructed tracks would either confirm the prediction of the electronic detector or act as veto and thus trigger the extraction of neighbouring bricks. In case of positive outcome, the brick emulsion films were developed and analysed. CS tracks were then matched with those reconstructed in the downstream films of the brick. These latter tracks were then followed upstream in the brick to their origins. Around the most upstream track disappearance point, a 1 cm^2 wide area in 10 downstream and 5 upstream emulsion films was scanned. All tracks and vertices in this volume were reconstructed, and short-lived particle decays were searched for. In case no neutrino interaction was found in the brick, the search would continue in less probable bricks. More details on the search and reconstruction of neutrino events in the bricks are given in [15–17].

3 Search for ν_e candidates

The brick acted as a high sampling calorimeter with more than five active layers every X_0 over a total thickness of 10 X_0. For most of ν_e CC interactions, the path of the electron in the brick is long enough for the electromagnetic (e.m.) shower to develop, thus allowing its detection and reconstruction in the emulsion films. On the other hand, the size of the standard scanned volume along the beam direction corresponds to about 1.8 X_0, which is too short for the e.m. shower to develop. The search for electrons is therefore performed in an extended scanned volume applying a dedicated procedure to the 0μ tagged events, i.e. events having no reconstructed three-dimensional muon track and less than 20 fired TT/RPC planes. A search is performed in the CS doublet for track segments less than 2 mm apart from the extrapolation point of each track originated from the interaction vertex (primary tracks). Moreover, the direction of candidate CS tracks is required to be compatible within 150 mrad with that of the primary track. If at least three tracks are found, additional scanning along the primary track is performed aiming at the detection of an e.m. shower [6].
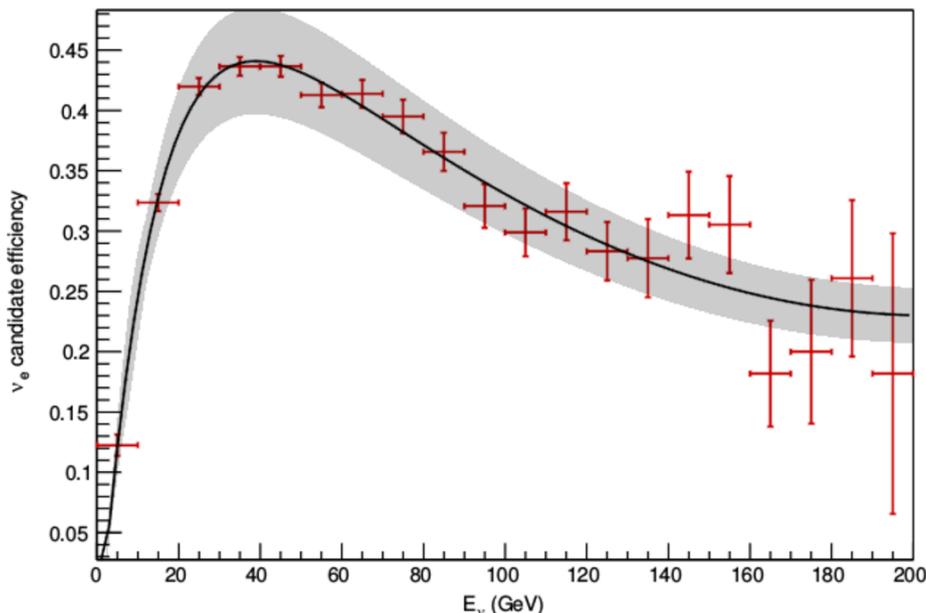
Figure 1. The ν_e CC candidate selection efficiency as a function of the neutrino energy. Error bars indicate the MC statistical errors. The black line is a fitted curve to the simulated efficiency points and the grey area represents the systematic error.

Detected showers are carefully inspected, by visual scan, in the first two films downstream the interaction vertex to assess whether they are produced by a single particle. Thanks to the high granularity of the OPERA nuclear emulsions, one can recognize an e-pair from γ conversion when the e-pair tracks are separated by more than 1 μm. Once the origin of the e.m. shower is confirmed as due to a single charged particle, the event is classified as ν_e candidate. A classifier algorithm [18], is applied to select neutrino interaction events fully contained in the fiducial volume of the detector.

The efficiency of the procedure applied to search for ν_e CC interactions, shown in figure 1, is computed by Monte Carlo (MC) simulation using the standard OPERA simulation framework [17]. Neutrino fluxes are determined by FLUKA [19, 20] based simulation of the CNGS beamline [21]. Neutrino interactions in the target are generated using the GENIE v2.8.6 generator [22, 23]. The simulated efficiency points are then fitted with an empirical function. Since the number of hit TT/RPC planes and presence of long tracks in neutrino events are correlated with the neutrino energy, as a result of 0μ tagging criterion, a drop in the efficiency is expected at high energies. In 2008–2012, the OPERA detector had collected data corresponding to 17.97×10^{19} p.o.t. In total, 19505 on-time events have been registered in the target volume. Out of them, 5868 events have a reconstructed neutrino interaction vertex in the first or second most probable brick and 1281 are tagged as 0μ events. The 0μ sample is further reduced to 1185 events by exclusion of not contained ones. In this sample the number of ν_e candidates is 35.

The number, N_{beam}, of ν_e candidates from CC interactions of ν_e and $\bar{\nu}_e$ beam components is estimated using a data-driven approach from the number of observed events with

	$R^j_{\nu_i} \quad (\langle \varepsilon^{0l}_j(\nu_i)\rangle)$			
	$j = CC$		$j = NC$	
$i = \mu$	640.4	(0.029)	215.2	(0.296)
$i = e$	5.9	(0.078)	2.2	(0.307)

Table 1. Expected rates of neutrino and antineutrino of type i interacting by the j process normalized to 10^{19} p.o.t. and 1 kt target mass. In brackets the efficiencies of ν_i interactions, convoluted with the CNGS ν_i flux and its j-type interaction cross sections, to be reconstructed as a $0l$ event.

no charged leptons, $0l$, which are 0μ events not identified as ν_e candidates, $n_{0l} = 1185-35$, according to:

$$N_{\text{beam}} = n_{0l} \frac{R^{CC}_{\nu_e} \langle \varepsilon^{\nu_e}_{CC}(\nu_e)\rangle}{\sum\limits_{i=\mu,e} \sum\limits_{j=CC,NC} R^j_{\nu_i} \langle \varepsilon^{0l}_j(\nu_i)\rangle}, \tag{3.1}$$

where $\langle \varepsilon^{\nu_e}_j(\nu_i)\rangle$ and $\langle \varepsilon^{0l}_j(\nu_i)\rangle$ are the efficiencies for the ν_i interactions ($i = \mu, e$), convoluted with the CNGS ν_i flux, ϕ_{ν_i}, and its j-type interaction cross sections, $\sigma^j_{\nu_i}$ (j = CC or NC), to be reconstructed as a ν_e candidate or as a $0l$ event, respectively, i.e.:

$$\langle \varepsilon^{\nu_e(0l)}_j(\nu_i)\rangle = \int \phi_{\nu_i} \varepsilon^{\nu_e(0l)}_j \sigma^j_{\nu_i} \, dE \left/ \int \phi_{\nu_i} \sigma^j_{\nu_i} \, dE \right., \tag{3.2}$$

while $R^j_{\nu_i}$ are the interaction rates of neutrino and antineutrino:

$$R^j_{\nu_i} = \int \phi_{\nu_i} \sigma^j_{\nu_i} \, dE. \tag{3.3}$$

The expected rates $R^j_{\nu_i}$, for 10^{19} p.o.t. and 1 kt target mass, and the efficiencies $\langle \varepsilon^{0l}_{CC}(\nu_i)\rangle$ are reported in table 1. The efficiency $\langle \varepsilon^{\nu_e}_{CC}(\nu_e)\rangle$ is 0.375.

The combined systematic error from flux normalization, ν_e/ν_μ flux ratio, detection efficiencies and cross section uncertainties is conservatively estimated as 20% and 10% for neutrino energies below and above $10\,\text{GeV}$, respectively. The expected value of N_{beam} amounts to 30.7 ± 0.9 (stat.) ± 3.1 (syst.) events. The expected numbers obtained with the above mentioned procedure are insensitive to systematic effects on the efficiencies up to the location level being common to ν_e and $0l$ events.

Background contributions are: ν_τ CC interactions with $\tau \to e$ decays, 0μ events with $\pi^0 \to \gamma\gamma$ decay with prompt γ conversion, and the electron-positron pair misidentified as an electron. The first type of background arises when the τ-lepton and its daughter electron track cannot be distinguished. It is estimated by MC simulation assuming the 3-flavour $\nu_\mu \to \nu_\tau$ oscillation scheme and oscillation parameters from [24]. It amounts to 0.7 ± 0.2 (syst.) events.

The background due to π^0 is derived from the data by counting the number of events fulfilling the criteria for a ν_e candidate with a γ converting in the second or third lead plate downstream of the interaction vertex. That number is converted into the probability to
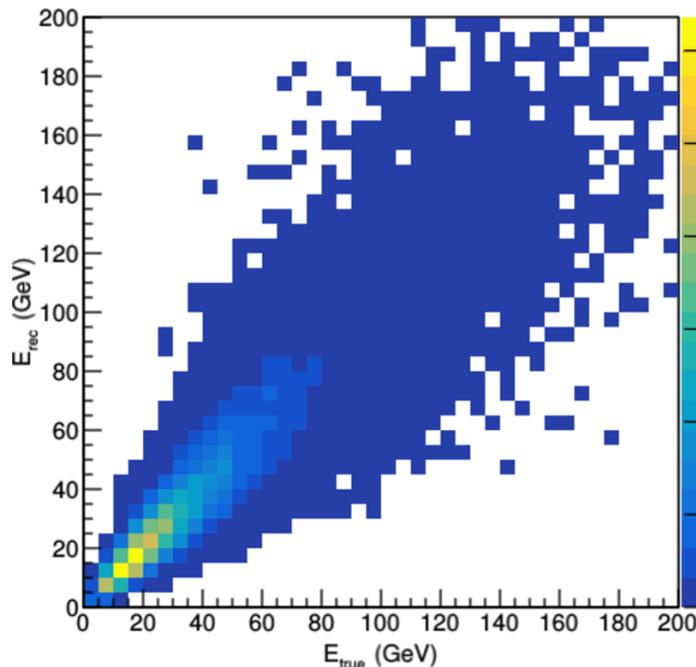
Figure 2. Reconstructed versus MC energy for ν_e CC events in the OPERA Target Trackers.

observe background ν_e candidates due to γ conversions in the first lead plate, taking into account the radiation length [6]. We expect 0.5 ± 0.5 (stat.) such events.

Summarizing, the expected number of background events, N_{bkg}, amounts to 1.2 ± 0.5 (stat.) ± 0.2 (syst.), while the sum of expected events from ν_e and $\bar{\nu}_e$ beam components and backgrounds is 31.9 ± 1.0 (stat.) ± 3.1 (syst.).

4 Energy reconstruction

The longitudinal and transverse development of e.m. showers are well parametrised both for homogeneous and sampling calorimeters [25–27], hence the energy shape analysis can be used to improve the electron energy reconstruction. The e.m. shower shape parametrisation together with the knowledge of the interaction vertex position and of the direction of the electron, obtained from the emulsion data, are the basis of the method applied in this analysis, as detailed in [28]. In this approach, the TT signals from e.m. shower, initiated by the electron at the interaction vertex, and the hadronic shower are separated. The hadronic shower energy is estimated by the calorimetric measurement in the TT. The electron energy is assessed by the shape analysis of the e.m. shower profiles. The reconstructed energy of ν_e CC events versus their true energy is shown in figure 2. The accuracy of the energy reconstruction of ν_e CC events can be parametrized as:

$$\frac{\Delta E}{E} = 0.18 + \frac{0.55}{\sqrt{E(\mathrm{GeV})}} \tag{4.1}$$

which is improved with respect to previous analysis [6].

5 Neutrino oscillation analysis

5.1 The 3 neutrino flavour mixing model

The neutrino oscillation phenomenon can lead to a non null difference, $n_{\rm osc}$, between the number of observed ν_e candidates, $n_{\rm obs}$, and that expected from the beam contamination, $N_{\rm beam}$ and from background, $N_{\rm bkg}$, i.e.

$$n_{\rm osc} = n_{\rm obs} - N_{\rm beam} - N_{\rm bkg}. \tag{5.1}$$

On the other end, assuming only contributions from $\nu_\mu(\bar{\nu}_\mu) \to \nu_e(\bar{\nu}_e)$ oscillations the expected value of ν_e candidates from oscillations, $N_{\rm osc}$, is:

$$N_{\rm osc} = k \cdot \int \phi_{\nu_\mu} P_{\mu e} \sigma_{\nu_e} \varepsilon_{\nu_e} dE, \tag{5.2}$$

where k is the averaged number of nuclei over the data taking period, $P_{\mu e}$ is the oscillation probability, ε_{ν_e} and σ_{ν_e} are the ν_e detection efficiency and cross section, respectively, ϕ_{ν_μ} is the ν_μ integrated flux and E is the neutrino energy. The average appearance probability, $\langle P_{\mu e} \rangle$, can be derived as:

$$\langle P_{\mu e} \rangle = \frac{n_{\rm osc}}{k \cdot \int \phi_{\nu_\mu} \sigma_{\nu_e} \varepsilon_{\nu_e} dE}. \tag{5.3}$$

An optimal interval on neutrino energy, 0–40 GeV, was introduced in order to maximize the sensitivity on the average appearance probability. $\langle P_{\mu e} \rangle$ is model-independent, and energy interval defined above can be used for any oscillation analysis of the OPERA data not based on the energy shape analysis. The 90% C.L. upper limit, obtained using the Feldman and Cousins method (F&C) [29], is $\langle P_{\mu e} \rangle < 3.5 \times 10^{-3}$ for neutrino energies $0 < E_\nu < 40$ GeV. A similar result, $\langle P_{\mu e} \rangle < 3.7 \times 10^{-3}$, is obtained using the Bayesian technique [30].

Constraints on the oscillation parameters are derived within the framework of the 3 neutrino flavour oscillation model. The expected number of ν_e candidates ($N_{3\nu}^{exp}$) depends on the disappearance of ν_e ($\bar{\nu}_e$) beam contamination and on ν_e ($\bar{\nu}_e$) appearance from ν_μ ($\bar{\nu}_\mu$) beam components. Both these contributions are taken into account. The oscillation probabilities are evaluated from:

$$P(\nu_\alpha \to \nu_\beta) = \delta_{\alpha\beta} - 4\sum_{i>j}(U_{\alpha i}U_{\beta i}U_{\alpha j}U_{\beta j})\sin^2\left(1.27\,\Delta m_{ij}^2\left({\rm eV}^2/c^4\right)\frac{L({\rm km})}{E({\rm GeV})}\right). \tag{5.4}$$

Using the standard parametrization of the mixing matrix U, the values of θ_{13}, θ_{23}, δ_{CP} and Δm_{ij}^2 from [24], the expected number of ν_e candidates, including 1.2 background events, is $N_{3\nu}^{exp} = 34.3 \pm 1.0$ (stat.) ± 3.4 (syst.). Matter effects are taken into account, more details are given in section 5.2. $N_{3\nu}^{exp}$ is consistent with 35 observed ν_e candidate events. Figure 3(a) shows the energy distributions of observed events, of the expectation from ν_e and $\bar{\nu}_e$ beam components, assuming no oscillations, and of background events (π^0 and $\tau \to e$). In figure 3(b) the energy distribution of observed events is compared with the expectation from $\nu_e(\bar{\nu}_e) \to \nu_e(\bar{\nu}_e)$ and $\nu_\mu(\bar{\nu}_\mu) \to \nu_e(\bar{\nu}_e)$ oscillations channels, and from background components. The background components, π_0 and $\tau \to e$, are assumed to be unaffected by oscillations. In the optimized neutrino energy range (0–40 GeV), the 90% C.L. upper limit on $\sin^2 2\theta_{13}$ is 0.43.
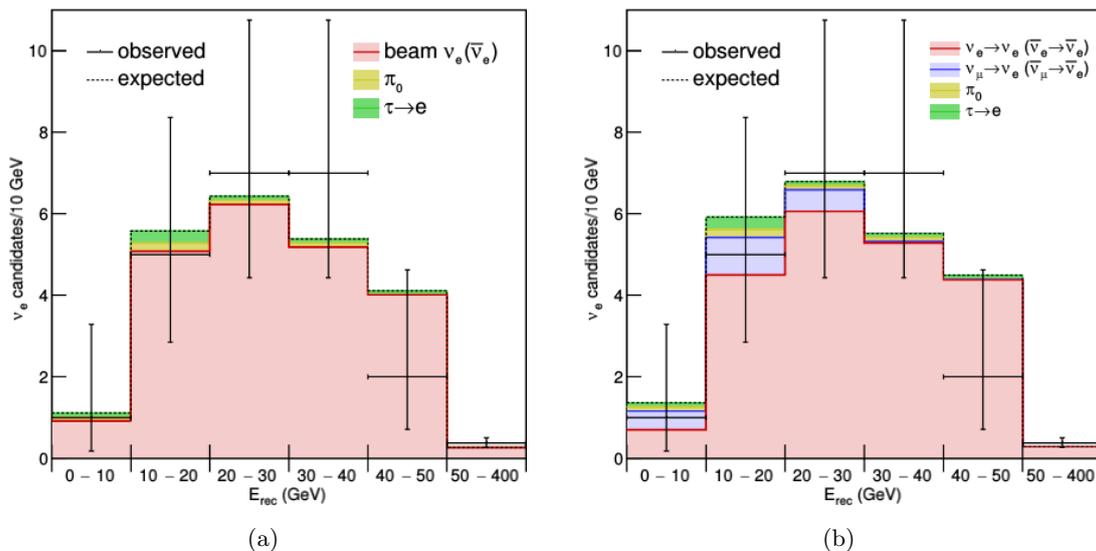
Figure 3. The reconstructed energy distributions of the observed ν_e candidates, the expected background and beam ν_e and $\bar{\nu}_e$ components: (a) assuming no oscillations; (b) in case of 3 neutrino flavour mixing with the parameters from [24].

5.2 Analysis in the 3+1 neutrino mixing model

The excess of ν_e and $\bar{\nu}_e$ reported by the LSND [7], MiniBooNE [8], reactor [9] and radio-chemical [10, 11] experiments may be interpreted as due to the presence of light, $\mathcal{O}(1\,\text{eV}/c^2)$, sterile neutrinos. OPERA can test the hypothesis of the presence of a sterile neutrino by comparing the observed ν_e energy spectrum with that predicted from the 3+1 neutrino mixing model. The event energy spectrum is divided in $N = 6$ bins, as shown in figure 3(a); n_i is the number of observed events in the i-th bin. The expected number of events in each bin, μ_i, is evaluated using GLoBES [34, 35]. Detector effects are taken into account by smearing matrices calculated by MC simulation. The contributions from four neutrino oscillation channels are taken into account, namely $\nu_e(\bar{\nu}_e) \to \nu_e(\bar{\nu}_e)$ and $\nu_\mu(\bar{\nu}_\mu) \to \nu_e(\bar{\nu}_e)$. The backgrounds arising from π^0 and $\tau \to e$, defined in section 3, are considered independent of the 3+1 mixing model parameters. Two corrective and independent factors, k_j ($j = 1, 2$), are introduced to take into account the overall systematic uncertainties, σ_j, on the intrinsic ν_e and $\bar{\nu}_e$ beam components, on the ν_e detection efficiency and on ν_e and $\bar{\nu}_e$ cross sections. The expected number of events is

$$\mu_i = \mu_i^0(1 + k_j) \quad \text{where} \quad \begin{cases} j = 1, & \text{if } i = 1 \\ j = 2, & \text{otherwise} \end{cases}. \tag{5.5}$$

μ_i^0 is the expected number of events estimated using the nominal fluxes, cross-sections and detection efficiencies. As already stated, the systematic uncertainties, σ_j, are conservatively estimated as 20% for the first energy bin ($E \leq 10\,\text{GeV}$) and 10% for $E > 10\,\text{GeV}$. The

profile likelihood ratio was used as test statistic, with the likelihood defined as:

$$-2\ln L = -2\sum_{i}^{N}\left(n_i\ln\mu_i - N\mu_i\right) + \sum_{j=1}^{2}\frac{k_j^2}{\sigma_j^2} + \frac{\left(\Delta m_{31}^2 - \widehat{\Delta m_{31}^2}\right)^2}{\sigma_{\Delta m_{31}^2}^2}. \qquad (5.6)$$

The last term is a penalty term accounting for the current knowledge on Δm_{31}^2 [24], $\widehat{\Delta m_{31}^2}$ and $\sigma_{\Delta m_{31}^2}^2$ are the best fit value and the 1σ uncertainty, respectively. The parameters of interest are the squared mass difference Δm_{41}^2 and the effective mixing $\sin^2 2\theta_{\mu e} = 4|U_{e4}|^2|U_{\mu 4}|^2$. It is worth noting that this definition of the effective mixing allows a direct comparison of this analysis with short-baseline results. The non-zero value of Δm_{21}^2 is taken into account as well as matter effects assuming a constant Earth crust density estimated with the PREM [36, 37] onion shell model. All other oscillation parameters are treated as nuisance parameters and profiled out. The result is restricted to positive Δm_{41}^2 values since negative values are disfavoured by results on the sum of neutrino masses from cosmological surveys [38]. The resulting 90% C.L. exclusion region is shown in figure 4. An upper limit on $\sin^2(2\theta_{\mu e}) = 0.021$ is set for $\Delta m_{41}^2 > 0.1$ eV^2. Moreover, OPERA contributes to limit the effective mixing for low Δm_{41}^2 and excludes $\Delta m_{41}^2 \gtrsim 4 \times 10^{-3}$ eV^2 for maximal mixing. It must be stressed that, for small Δm_{41}^2 values, OPERA is the only experiment having collected data in appearance mode. MINOS and Daya Bay/Bugey-3 have obtained a more stringent exclusion limit in a combined analysis of their disappearance results on, respectively, an accelerator ν_μ beam and reactors $\bar{\nu}_e$ fluxes.

6 Conclusions

The full OPERA data sample collected during the 2008–2012 CNGS beam runs is used to search for ν_e candidates. Compared to the previous search [6], results reported here are based on a larger statistics and improved ν_e CC energy resolution. Model independent results are reported to allow testing different oscillation hypotheses. The results are compatible with the no-oscillation hypothesis as well as with the 3 neutrino flavour one. In the latter case, a 90% C.L. upper limit $\sin^2(2\theta_{13}) < 0.43$ is set. For the first time, in this paper, the results are also analysed in a 3+1 model to test the hypothesis of the existence of a sterile neutrino as suggested by several experiments. A 90% C.L. upper limit $\sin^2(2\theta_{\mu e}) = 0.021$ for $\Delta m_{41}^2 \gtrsim 0.1\,\text{eV}^2$ is set, thus excluding a sizable part of the region hinted by LSND and MiniBooNE experiments. OPERA is the only appearance experiment excluding neutrino mass difference down to $4 \times 10^{-3}\,\text{eV}^2$.
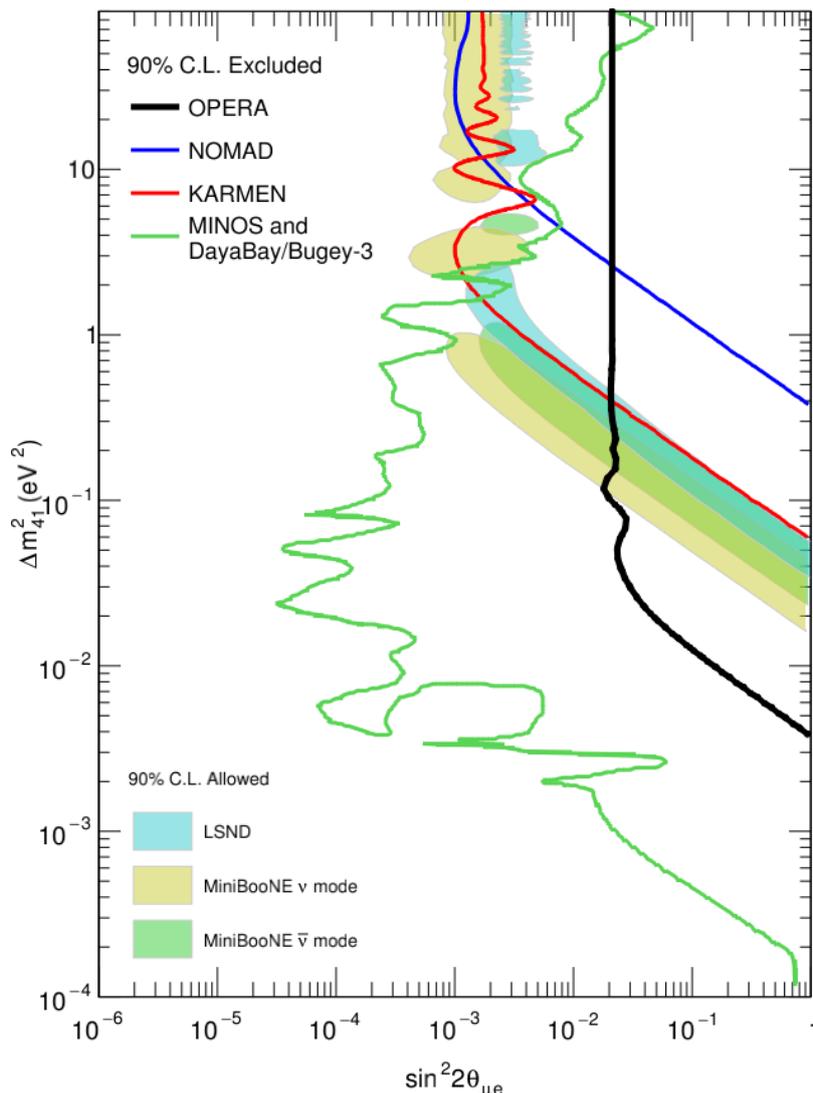
Acknowledgments

Figure 4.   The 90% C.L. exclusion plot in the Δm_{41}^2 and $\sin^2 2\theta_{\mu e}$ plane is shown (black line) together with the 90% C.L. allowed region obtained by LSND (cyan) and MiniBooNE (yellow and green for ν and $\bar{\nu}$ mode, respectively). The blue, red and green lines represent the 90% C.L. exclusion regions obtained by NOMAD [31], KARMEN [32] and the MINOS and DayaBay/Bugey-3 joint analysis [33], respectively.

References

[1] OPERA collaboration, M. Guler at al., *An appearance experiment to search for $\nu_\mu \leftrightarrow \nu_\tau$ oscillations in the CNGS beam. Experimental proposal*, SPSC-2000-028 (2000) [CERN-SPSC-P-318] [LNGS-P25-00].

[2] R. Acquafredda et al., *The OPERA experiment in the CERN to Gran Sasso neutrino beam*, 2009 *JINST* **4** P04018 [INSPIRE].

[3] G. Acquistapace et al., *The CERN neutrino beam to Gran Sasso (NGS)*, CERN-98-02 (1998) [INFN/AE-98/05].

[4] R. Bailey et al., *The CERN neutrino beam to Gran Sasso (NGS). Addendum to report CERN-98-02, INFN/AE-98/05*, CERN-SL/99-034(DI) (1999) [INFN/AE-99/05].

[5] OPERA collaboration, N. Agafonova et al., *Discovery of τ neutrino appearance in the CNGS neutrino beam with the OPERA experiment*, *Phys. Rev. Lett.* **115** (2015) 121802 [arXiv:1507.01417] [INSPIRE].

[6] OPERA collaboration, N. Agafonova et al., *Search for $\nu_\mu \to \nu_e$ oscillations with the OPERA experiment in the CNGS beam*, *JHEP* **07** (2013) 004 [arXiv:1303.3953] [INSPIRE].

[7] LSND collaboration, A. Aguilar et al., *Evidence for neutrino oscillations from the observation of anti-neutrino(electron) appearance in a anti-neutrino(muon) beam*, *Phys. Rev.* **D 64** (2001) 112007 [hep-ex/0104049] [INSPIRE].

[8] MiniBooNE collaboration, A.A. Aguilar-Arevalo et al., *A combined $\nu_\mu \to \nu_e$ and $\bar{\nu}_\mu \to \bar{\nu}_e$ oscillation analysis of the MiniBooNE excesses*, arXiv:1207.4809 [FERMILAB-PUB-12-394-AD-PPD] [LA-UR-12-23041].

[9] G. Mention et al., *The reactor antineutrino anomaly*, *Phys. Rev.* **D 83** (2011) 073006 [arXiv:1101.2755] [INSPIRE].

[10] F. Kaether et al., *Reanalysis of the GALLEX solar neutrino flux and source experiments*, *Phys. Lett.* **B 685** (2010) 47 [arXiv:1001.2731] [INSPIRE].

[11] J.N. Abdurashitov et al., *Measurement of the response of a Ga solar neutrino experiment to neutrinos from an Ar-37 source*, *Phys. Rev.* **C 73** (2006) 045805 [nucl-ex/0512041] [INSPIRE].

[12] K. Niu, E. Mikumo and Y. Maeda, *A possible decay in flight of a new type particle*, *Prog. Theor. Phys.* **46** (1971) 1644 [INSPIRE].

[13] OPERA collaboration, N. Agafonova et al., *Determination of the muon charge sign with the dipolar spectrometers of the OPERA experiment*, 2016 *JINST* **11** P07022 [arXiv:1404.5933] [INSPIRE].

[14] Y.A. Gornushkin, S.G. Dmitrievsky and A.V. Chukanov, *Locating of the neutrino interaction vertex with the help of electronic detectors in the OPERA experiment*, *Phys. Part. Nucl. Lett.* **12** (2015) 89.

[15] OPERA collaboration, N. Agafonova et al., *Observation of a first ν_τ candidate in the OPERA experiment in the CNGS beam*, *Phys. Lett.* **B 691** (2010) 138 [arXiv:1006.1623] [INSPIRE].

[16] OPERA collaboration, N. Agafonova et al., *Procedure for short-lived particle detection in the OPERA experiment and its application to charm decays*, *Eur. Phys. J.* **C 74** (2014) 2986 [arXiv:1404.4357] [INSPIRE].

[17] OPERA collaboration, N. Agafonova et al., *New results on $\nu_\mu \to \nu_\tau$ appearance with the OPERA experiment in the CNGS beam*, *JHEP* **11** (2013) 036 [*Erratum ibid.* **04** (2014) 014] [arXiv:1308.2553] [INSPIRE].

[18] A. Bertolin and N.T. Tran., *OpCarac: an algorithm for the classification of the neutrino interactions recorded by the OPERA experiment*, OPERA public note 100 (2009).

[19] T.T. Böhlen et al., *The FLUKA code: developments and challenges for high energy and medical applications*, *Nucl. Data Sheets* **120** (2014) 211.

[20] A. Ferrari, P. R. Sala, A. Fasso and J. Ranft, *FLUKA: A multi-particle transport code*, CERN-2005-010 (2005) [SLAC-R-773] [INFN-TC-05-11].

[21] CNGS web site, http://proj-cngs.web.cern.ch/proj-cngs.

[22] C. Andreopoulos et al., *The GENIE neutrino Monte Carlo generator*, *Nucl. Instrum. Meth.* **A 614** (2010) 87 [arXiv:0905.2517] [INSPIRE].

[23] C. Andreopoulos et al., *The GENIE neutrino Monte Carlo generator: physics and user manual*, arXiv:1510.05494 [INSPIRE].

[24] PARTICLE DATA GROUP collaboration, C. Patrignani et al., *Review of particle physics*, *Chin. Phys.* **C 40** (2016) 100001 [INSPIRE].

[25] E. Longo and I. Sestili, *Monte Carlo calculation of photon initiated electromagnetic showers in lead glass*, *Nucl. Instrum. Meth.* **128** (1975) 283 [*Erratum ibid.* **135** (1976) 587] [INSPIRE].

[26] G. Grindhammer and S. Peters, *The parameterized simulation of electromagnetic shower in homogeneous and sampling calorimeters*, hep-ex/0001020.

[27] C. Leroy and P. Rancoita, *Physics of cascading shower generation and propagation in matter: Principles of high-energy, ultrahigh-energy and compensating calorimetry*, *Rept. Prog. Phys.* **63** (2000) 505 [INSPIRE].

[28] S. Zemskova, *$\nu_\mu \to \nu_e$ oscillations search in the OPERA experiment*, *Phys. Part. Nucl.* **47** (2016) 1003 [INSPIRE].

[29] G.J. Feldman and R.D. Cousins, *A Unified approach to the classical statistical analysis of small signals*, *Phys. Rev.* **D 57** (1998) 3873 [physics/9711021] [INSPIRE].

[30] G. Cowan, *Statistical data analysis*, Clarendon Press, Oxford U.K. (1998).

[31] NOMAD collaboration, P. Astier et al., *Search for $\nu_\mu \to \nu_e$ oscillations in the NOMAD experiment*, *Phys. Lett.* **B 570** (2003) 19 [hep-ex/0306037] [INSPIRE].

[32] KARMEN collaboration, B. Armbruster et al., *Upper limits for neutrino oscillations $\bar{\nu}_\mu \to \bar{\nu}_e$ from muon decay at rest*, *Phys. Rev.* **D 65** (2002) 112001 [hep-ex/0203021] [INSPIRE].

[33] MINOS, Daya Bay collaboration, P. Adamson et al., *Limits on active to sterile neutrino oscillations from disappearance searches in the MINOS, Daya Bay and Bugey-3 experiments*, *Phys. Rev. Lett.* **117** (2016) 151801 [arXiv:1607.01177] [INSPIRE].

[34] P. Huber, M. Lindner and W. Winter, *Simulation of long-baseline neutrino oscillation experiments with GLoBES (General Long Baseline Experiment Simulator)*, *Comput. Phys. Commun.* **167** (2005) 195 [hep-ph/0407333] [INSPIRE].

[35] P. Huber, J. Kopp, M. Lindner, M. Rolinec and W. Winter, *New features in the simulation of neutrino oscillation experiments with GLoBES 3.0: General Long Baseline Experiment Simulator*, *Comput. Phys. Commun.* **177** (2007) 432 [hep-ph/0701187] [INSPIRE].

[36] A.M. Dziewonski and D.L. Anderson, *Preliminary reference Earth model*, *Phys. Earth Planet. Interiors* **25** (1981) 297.

[37] F.D. Stacey and P.M. Davis, *Physics of the Earth*, 4$^{\text{th}}$ edition, Cambridge University Press, Cambridge U.K. (2008).

[38] Planck collaboration, P.A.R. Ade et al., *Planck 2015 results. XIII. Cosmological parameters*, *Astron. Astrophys.* **594** (2016) A13 [arXiv:1502.01589] [INSPIRE].